First published in:
APPLIED PHYSICS LETTERS VOLUME 85, NUMBER 11 13 SEPTEMBER 2004

Direct laser writing and characterization of "Slanted Pore" Photonic Crystals

Markus Deubel[a)]
Institut für Nanotechnologie, Forschungszentrum Karlsruhe in der Helmholtz-Gemeinschaft, Postfach 3640, D-76021 Karlsruhe, Germany

Martin Wegener
Institut für Angewandte Physik, Wolfgang-Gaede-Straße 1, Universität Karlsruhe (TH), D-76131 Karlsruhe, Germany

Artan Kaso and Sajeev John
Department of Physics, University of Toronto, 60 St. George Street, Toronto, Ontario M5S 1A7, Canada

(Received 30 March 2004; accepted 21 June 2004)

We report the fabrication and characterization of the recently proposed Slanted Pore Photonic Crystals. The Photonic Crystals fabricated via direct laser writing by multiphoton polymerization are characterized by electron microscopy as well as by optical spectroscopy. The latter is compared with band structure calculations. We show that this Slanted Pore geometry allows for controlling the surface termination of the Photonic Crystal. © *2004 American Institute of Physics*.
[DOI: 10.1063/1.1792802]

After the invention of the concept of Photonic Crystals (PCs) and photonic band gap (PBG) materials[1,2] a new era of advanced nanomaterials for photonics and telecommunication has begun. Still, the search for the "ideal" structure of three-dimensional PBG materials is ongoing. One obvious goal is to obtain a complete PBG at low refractive index contrast or to optimize the size of the gap for a given index contrast, e.g., that of silicon and air. In 1994, the group of Soukoulis proposed the layer-by-layer or woodpile structure which exhibits a complete PBG of up to 25% of the midgap frequency for silicon/air.[3] This structure is accessible by a variety of experimental approaches and has been investigated intensively throughout the last decade.[4–7] A more general class of PCs are the so-called "SP_2" structures from the family of tetragonal Slanted Pore PCs, proposed only very recently.[8] For orthogonal pores and special parameters, the SP_2 PC reduces to a rotated woodpile structure but it offers new approaches and opportunities for fabrication. Importantly, the SP_2 PBG is extremely robust against fabrication induced structural errors.

In this letter, we demonstrate the experimental realization of Slanted Pore PCs.Employing the technique of direct laser writing (DLW) by multiphoton polymerization,[9] we achieve lattice constants which are roughly compatible with the requirements for operation at telecommunication wavelengths. Electron micrographs as well as optical characterization reveal excellent quality. Importantly, the Slanted Pore structure is particularly well-suited for the technique of direct laser writing for two reasons: (i) Due to the orientation of the structure with respect to the photoresist layer, more symmetrical rods can be fabricated. (ii) Due to the same reason, the surface termination of the three-dimensional PC can be controlled. (Both are not possible in woodpile-type structures fabricated via DLW.[10,11]) A proof-of-principle for this aspect is also given. The ability to tailor the surface termination potentially allows for controlling the coupling of the electromagnetic field from air into the PC in detail.

Slanted Pore structures of two pores per direct lattice point (SP_2), denoted as $S/[n_1,n_2]\oplus[m_1,m_2]^{(\delta_1,\delta_2)}$ (where S stands for square), can be understood as two tetragonal sublattices, each with primitive vectors $\boldsymbol{a}_1$, $\boldsymbol{a}_2$, and $\boldsymbol{c}$, superposed to create a single tetragonal lattice with primitive vectors $\boldsymbol{a}_1$, $\boldsymbol{a}_2$,and $\boldsymbol{c}$. The second sublattice is displaced by a vector $\boldsymbol{\delta}=\delta_1\boldsymbol{a}_1+\delta_2\boldsymbol{a}_2$, where $0\leqslant\delta_1,\delta_2\leqslant 1$, from the first. For each sublattice there is only one pore associated with every single lattice point. For the first sublattice the pore runs from 0 to $n_1\boldsymbol{a}_1+n_2\boldsymbol{a}_2+1\boldsymbol{c}$, while for the second sublattice the pore runs from $\delta_1\boldsymbol{a}_1+\delta_2\boldsymbol{a}_2$ to $(\delta_1+m_1)\boldsymbol{a}_1+(\delta_2+m_2)\boldsymbol{a}_2+1\boldsymbol{c}$. The pore can be thought of as a rod of radius r. Varying $|\boldsymbol{c}|,\delta_1,\delta_2,r$ with respect to $|\boldsymbol{a}_1|=|\boldsymbol{a}_2|=a$, an optimized structure for a maximal PBG can be obtained.

Due to the simple geometrical architecture consisting of straight rods, the Slanted Pore PCs are ideal structures for fabrication via DLW. As a photoresist, we choose the commercially available thick film negative photoresist SU-8 (MicroChem). SU-8 is a chemically amplified negative photoresist that cures by cationic polymerization: Upon irradiation by near-UV light, the photoinitiator creates an acid, and only in a postexposure bake, this acid catalyzes the cross linking reaction of the monomers to the polymer. Insufficiently cross linked photoresist in underexposed regions is washed out by a solvent in a following development step. For DLW, the cationic polymerization mechanism is advantageous compared to photoresists working with radical polymerization, since the difference in the refractive index change during exposure is negligible, and already exposed structures will not affect further exposure steps. Another advantage is that SU-8 is solid during exposure, hence exposed structures do not need to be interconnected immediately.

For our experiments, 20-μm-thick solid SU-8 films are prepared by spin coating the photoresist on microscope cover slides followed by a soft bake step. To fabricate PC structures in such films, we use a regeneratively amplified Ti:sapphire laser system (Spectra Physics Hurricane). The laser system provides 120 fs pulses at a repetition rate adjustable from 1 kHz to single shot mode and a central wavelength of

a)Electronic mail: markus.deubel@physik.uni-karlsruhe.de

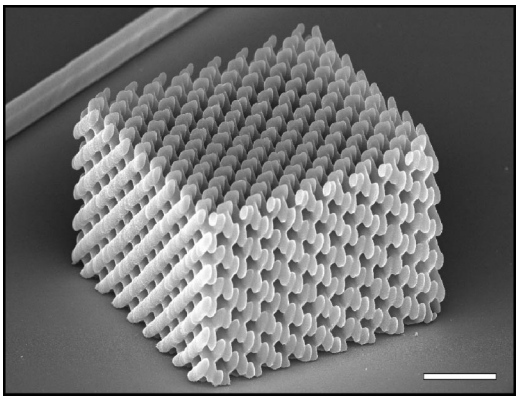

FIG. 1. Slanted Pore Photonic Crystal of the $S/[1,1]\oplus[-1,-1]^{(0.5,0)}$ family with $a=1.0$ μm, $c=1.41$ μm, fabricated by DLW. Scale bar: 3 μm.

800 nm, where the one-photon absorption of the photoresist is negligible. The output beam is attenuated by a half-wave plate/polarizer combination, and after beam expansion, typically a few tens of nanojoules of single pulse energy are focused into the photoresist sample by the 100× oil immersion objective (Leica, numerical aperture NA=1.4) of an inverted microscope (Leica). The sample is placed on a three-axis piezo scanning stage (Physik Instrumente) that provides a resolution of 5 nm at a full scanning range of 200 μm $\times 200$ μm $\times 20$ μm. A personal computer controls the scanning operation of the piezo and synchronizes its movement with the output of the laser system. After DLW of the preprogrammed pattern, the exposed sample is postbaked and developed, resulting in a positive image of the scanned pattern.

From the SP_2 PC architectures described above, we choose the $S/[1,1]\oplus[-1,-1]^{(0.5,0)}$ structure for fabrication by DLW, as this geometry can have a full PBG of up to 24% for air rods in a silicon background.[8] When fabricated by DLW, the samples consist of SU-8 rods in air. These rods are built up from voxels that are exposed by a single laser pulse each. The near-ellipsoidal shape of the voxels is determined by the employed wavelength λ and the NA of the microscope objective. For $\lambda=800$ nm and NA=1.4, a near-elliptical cross section with an aspect ratio (axial diameter/lateral diameter) of about 2.7 is expected, where the absolute dimension can be adjusted by the single pulse energy of the laser light. Within the rods, these voxels are arranged with their axes tilted by 45° with respect to the rod axis, resulting in a near-elliptical rod cross section with an aspect ratio of only about 1.9.

The $S/[1,1]\oplus[-1,-1]^{(0.5,0)}$ PCs that we fabricate have a tetragonal unit cell with $a=1.0$ μm and $c=1.41$ μm. The rod diameter is adjusted to about 360 nm so that rods of adjacent layers touch to give the structure mechanical stability. Figure 1 shows a scanning electron microscope image of a free-standing sample consisting of $8.5\times8.5\times5$ lattice constants. For optical characterization we fabricate larger samples with areas of 40 μm $\times 40$ μm that are surrounded by a massive wall in order to reduce lattice distortions and sample bending during development due to polymer shrinkage. Figure 2 shows the top view onto such a sample.

These samples are large enough for optical experiments as well as for potential devices. Transmission and reflection of the PCs are measured with a Fourier transform infrared spectrometer (Bruker, NIR halogen source) combined with an infrared microscope (Bruker, 36× Cassegrain objective, numerical aperture NA=0.5, liquid N_2-cooled InSb-detector/Si-photodiode). The samples are aligned with their surfaces perpendicular to the optical axis, which corresponds to Γ−Z direction of the $S/[1,1]\oplus[-1,-1]^{(0.5,0)}$ structure. A circular area with a diameter of 20 μm is defined by an aperture in the light path of the microscope. The transmission and reflection spectra are normalized to the bare cover slide and a silver mirror, respectively.

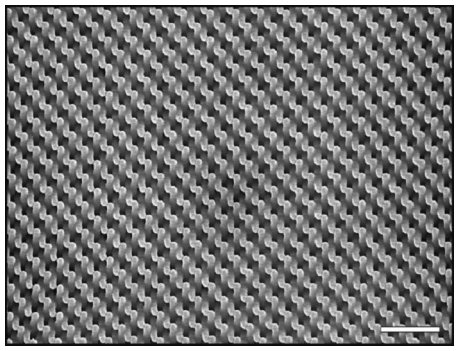

FIG. 2. Top view of a similar sample with a larger area as it is used for optical measurements. Scale bar: 3 μm.

Figure 3 shows transmission and reflection spectra for two different samples with a thickness of four and six lattice constants, respectively. The fundamental stop band around 1.8 μm wavelength is clearly visible as a pronounced dip in transmission and a peak in reflection. Higher order features around 0.9 μm are also visible, underlining the high optical quality of our samples. The overall roll-off toward shorter wavelengths is attributed to scattering.

Figure 4 compares the transmission spectrum of the sample with a thickness of six lattice constants with band structure calculations. The band structure is calculated using the plane wave expansion method for the ***H***-field. A total number of 1281 ***G*** vectors of the reciprocal lattice, whose length was shorter than a certain radius in reciprocal space, was used. The unit cell is considered to be the one shown as an inset of Fig. 4. Its parameters were chosen to be $a=1$, $c=\sqrt{2}$. The SU-8 content of the unit cell was mapped as follows: a mesh of $301\times301\times301$ points was set up; all mesh points were given the zero value; a voxel (ellipsoid of

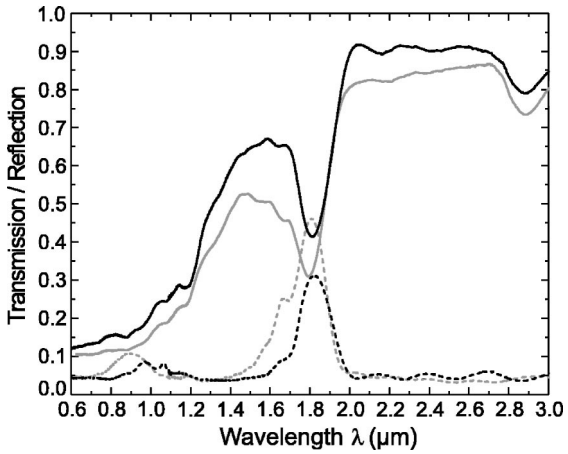

FIG. 3. Transmission (solid line) and reflection (dashed line) spectra of two samples with a thickness of four (black) and six (gray) lattice constants, respectively. The transmission dips above 2.9 μm wavelength stem from polymer absorption bands.

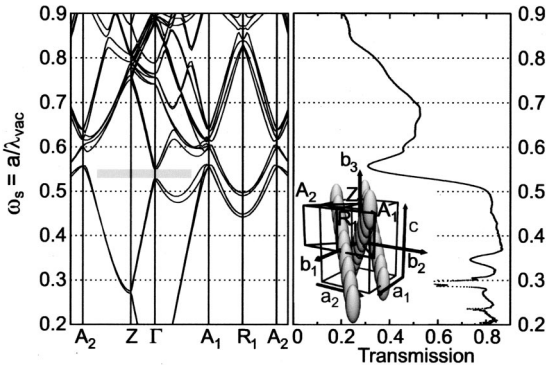

FIG. 4. Band structure calculations for the sample geometry shown in Figs. 1 and 2. $a=1.0$ μm. The right-hand side shows the transmission spectrum of the sample with a thickness of six lattice constants from Fig. 3.

revolution of semi-axes $X=Y=0.178$ a, $Z=2.7$ X) with its Z axis parallel to the c side of the unit cell, was moved inside the mesh, switching the mesh points it swept from zero to one; the mesh points with zero values are then associated with the dielectric background (air), while those with values of one are associated with the SU-8 content. By moving the voxel in small enough steps we can realize very smooth rods (limited only by the number of the mesh points). In the presented calculations nine voxels were aligned along the diagonal of the unit cell. The value $X=0.178$ a was chosen such as to have the SU-8 rods barely touching each other.

The position of the dip in transmission corresponds reasonably well with the stop band (outlined on the left-hand side of Fig. 4) expected from the band structure for $\Gamma-Z$ direction. The measured position of the dip is slightly displaced toward the higher frequencies. This can be associated with: the finite number of plane waves we use in the calculation; the filling fraction of the unit cell (the idealization made by approximating the DLW voxels with ellipsoids of revolution stacked with infinite resolution accuracy). When comparing the width and the position of the dip with the calculations, one has to be aware that the finite NA of the microscope objective corresponds to a spread of angles of incidence of up to 30° with respect to the sample surface normal. Thus, the measured spectra are an effective average over different directions. Together with the width of the stop band expected from Fig. 4, this leads to a broadening of the dip.[12]

With the high flexibility of the DLW approach, it is furthermore possible to custom design not only the PC structure, but also to tailor the *surface termination* of the PC. This potentially allows direct control of the coupling of the light from air to the PC and reduction in coupling losses for potential devices. Here we just give a proof-of-principle. Figure 5 shows two Slanted Pore PCs with different surface terminations, where sample (a) is higher by $c/8$ than sample (b).

In conclusion, we have realized and characterized Photonic Crystals from the SP_2 Slanted Pore family. Optical reflection and transmission data match closely with band structure calculations that take into account the discrete voxel structure of the SP_2 rods. PCs of this nature may be used as templates for PBG micro-fabrication through a double inversion procedure. The first step consists of room temperature chemical vapor deposition (CVD) of SiO_2 (Ref. 13) to surround the rods of the SU-8 PC, followed by burning away the SU-8 scaffolding. The resulting SiO_2 PC can subsequently be used as a daughter template for infiltration of silicon using high temperature CVD, followed by selective chemical etching (removal) of the SiO_2 scaffolding.[14] The silicon-based replica of the original polymer template is expected to exhibit a complete three-dimensional PBG[8].

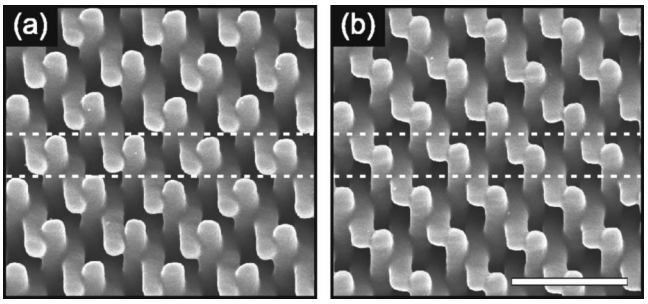

FIG. 5. Two Slanted Pore Photonic Crystals with $a=1.5$ μm which differ in the surface termination: (a) corresponds to the "X" configuration of the rods at the surface, (b) to the "Λ" configuration. Scale bar: 3 μm.

The authors acknowledge the support by the Center for Functional Nanostructures (CFN) of the Deutsche Forschungsgemeinschaft (DFG) within project A1.4, and the support of the Natural Sciences and Engineering Research Council of Canada. The research of M.W. is further supported by DFG-Project No. We 1497/9-1.

[1] E. Yablonovitch, Phys. Rev. Lett. **58**, 2059 (1987).
[2] S. John, Phys. Rev. Lett. **58**, 2486 (1987).
[3] K. M. Ho, C. T. Chan, C. M. Soukoulis, R. Biswas, and M. Sigalas, Solid State Commun. **89**, 413 (1994).
[4] E. Özbay, E. Michel, G. Tuttle, R. Biswas, M. Sigalas, and K.-M. Ho, Appl. Phys. Lett. **64**, 2059 (1994).
[5] S. Y. Lin, J. G. Fleming, D. L. Hetherington, B. K. Smith, R. Biswas, K. M. Ho, M. M. Sigalas, W. Zubrzycki, S. R. Kurtz, and J. Bur, Nature (London) **394**, 251 (1998).
[6] S. Noda, K. Tomoda, N. Yamamoto, and A. Chutinan, Science **289**, 604 (2000).
[7] K. Aoki, H. T. Miyazaki, H. Hirayama, K. Inoshita, T. Baba, K. Sakoda, N. Shinya, and Y. Aoyagi, Nat. Mater. **2**, 117 (2003).
[8] O. Toader, M. Berciu, and S. John, Phys. Rev. Lett. **90**, 233901 (2003).
[9] S. Maruo, O. Nakamura, and S. Kawata, Opt. Lett. **22**, 132 (1997).
[10] H.-B. Sun, S. Matsuo, and H. Misawa, Appl. Phys. Lett. **74**, 786 (1999).
[11] M. Straub and M. Gu, Opt. Lett. **27**, 1824 (2002).
[12] M. Deubel, G. von Freymann, M. Wegener, S. Pereira, K. Busch, and C. M. Soukoulis, Nat. Mater. **3**, 444 (2004).
[13] H. Miguez, N. Tétreault, B. Hatton, S. M. Yang, D. Perovic, and G. A. Ozin, Chem. Commun. (Cambridge) **22**, 2736 (2002).
[14] A. Blanco, E. Chomski, S. Grabtchak, M. Ibisate, S. John, S. W. Leonard, C. Lopez, F. Meseguer, H. Miguez, J. P. Mondia, G. A. Ozin, O. Toader, and H. M. van Driel, Nature (London) **405**, 437 (2000).